BAMS Article

Around the World They Go

Circumnavigating Balloon Satellites!

Todd McKinney, Nick Perlaky, Evan Danielson, Areeb Mohammed, Jackson Lee, Ben O'Bryan, Connor Stoll, Clara Hochmuth, Tyler Gallien, Skyler Kerr, Timothy Johnson, Chris Shiffer, Sean Hassler, Ethan Jankens, Mariama Feaster, Connor Morris, Zeb Leffler, Alice Crawford, Mark Cohen, Michael Newchurch, Bill Brown, Paula Tucker, and Kevin Knupp

ABSTRACT: Students from the University of Alabama in Huntsville successfully deployed three micro superpressure balloon satellites in winter 2021. Students planned and implemented all phases of the project: obtaining funding, determining project timelines, preparing equipment, launching balloons, designing and implementing a website, writing daily blogs on the balloon progress, and analyzing the data. The objective of the flights was to use the balloons as a meteorological tool to study conditions in the lower stratosphere (12–14 km), as a tracer for evaluating modeled air parcel trajectories, and as an outreach and educational tool. The three balloons successfully traveled hundreds of thousands of kilometers, making an accumulated total of 16 global circumnavigations. Throughout the project, students made connections with hundreds of researchers, ham radio operators, STEM groups, and other students around the globe. The balloons provided velocity telemetry within many different weather regimes, including vigorous jets over the Himalayas, slow-moving equatorial air masses over the middle of the Pacific Ocean, and dense polar air masses over the Arctic Circle. This study has found that the accuracy of HYSPLIT-calculated trajectories using numerical weather predication (NWP) meteorological data can be quantified using parcel velocity, duration of trajectory forecast, and spatial resolution of the NWP model.

KEYWORDS: Atmosphere; Lagrangian circulation/transport; Numerical analysis/modeling; Global transport modeling; Tracers; Education

https://doi.org/10.1175/BAMS-D-21-0135.1
Corresponding author: Todd McKinney, tm0155@uah.edu
In final form 3 August 2022
©2023 American Meteorological Society
For information regarding reuse of this content and general copyright information, consult the AMS Copyright Policy.

Brought to you by NOAA Central Library | Unauthenticated | Downloaded 07/19/23 04:33 PM UTC

AFFILIATIONS: McKinney—NOAA/Air Resources Laboratory, College Park, Maryland, and University of Alabama in Huntsville, Huntsville, Alabama; **Perlaky, Danielson, Mohammed, Lee, O'Bryan, Stoll, Hochmuth, Gallien, Kerr, Johnson, Shiffer, Hassler, Jankens, Feaster, Morris, Leffler, Newchurch, Tucker, and Knupp**—University of Alabama in Huntsville, Huntsville, Alabama; **Crawford and Cohen**—NOAA/Air Resources Laboratory, College Park, Maryland; **Brown**—NASA Marshall Space Flight Center, Huntsville, Alabama

Balloons capture the imagination. The ubiquity of using helium-filled balloons for celebrations means many people first encounter buoyant balloons as children and can remember watching a balloon magically and sometimes tragically soar off into the air. Balloons are popular with hobbyists, educators, and students who find that excellent resources with instructions on how to launch and track your own balloon are available and the equipment needed is affordable (Gilfort 2017). For many in this group, launching and tracking balloons is the main goal of the project. Launching and tracking a balloon requires knowledge of electronics, meteorology, radio, and physics. Studies have shown that students participating in science, technology, engineering, and math (STEM) extracurricular activities are more likely to remain in a STEM field, are more adaptable in team settings, and, on average, perform better in classes (Carpi et al. 2013; Peterman et al. 2016; Florence et al. 2018). Besides educational benefits, rewards for a successful launch can include connecting with others who share similar interests, obtaining cool pictures if a camera is part of the payload, the satisfaction of tracking your balloon to far-flung locations, or a fun road trip to recover a payload. As undergraduate students at University of Alabama Huntsville (UAH), we had another lofty goal for our balloon project. We wanted to show that the balloons we launched could be utilized as scientific instruments to help address current gaps in global high-altitude balloon data.

The application of high-altitude balloons (weather balloons) is an essential tool in atmospheric research. Data from balloons deployed from hundreds of sounding stations around the globe provide vertical profiles of important atmospheric variables. The balloons are designed to collect data as they ascend. Once they reach a certain altitude they burst. As stated by the U.S. National Oceanic and Atmospheric Administration (NOAA) National Weather Service (NWS), weather balloons "provide valuable input for computer forecast models, local data for meteorologists to make forecasts and predict storms, and data for research" (National Weather Service 2022). However, weather balloon data have their limits. Vast oceans and remote continental areas generally do not have sounding stations.

Unlike the balloons used for soundings, superpressure balloons are manufactured to withstand the outward-expanding pressure of the lifting gas inside the balloon. They rise and then stop at a certain altitude. Although the scientific value of data collected using superpressure balloons is well established (Cathey 2009; Friedrich et al. 2017), these balloons are not commonly used for daily meteorological observations. The balloons have tended to be extremely large, heavy, and in many cases require special machinery to deploy. The size and weight of these balloons makes flights only possible in certain regulated air space. In contrast, our group deployed micro superpressure balloons only about a meter long. To our knowledge, this is the first report of using such small balloons to collect a scientific dataset.

In the second section we give an overview of the project and some of the soft outcomes. Then we give technical details about the balloons and a description of the data collected in

Brought to you by NOAA Central Library | Unauthenticated | Downloaded 07/19/23 04:33 PM UTC

the third section. In the fourth and fifth sections we describe a simple yet informative analysis of airmass trajectories.

The project

In early 2021, under the auspices of the UAH Space Hardware Club, undergraduate students (see Fig. 1) planned a project to deploy five micro superpressure balloons with a payload that could collect useful data in areas inaccessible to weather balloons used in sounding stations and large superpressure balloons. Micro superpressure balloons are only about a meter long making them much smaller, easier to handle, and more affordable than the football-stadium-sized NASA superpressure balloons (Cathey 2009). They are popular among hobbyists and are often deployed and tracked for sheer fun or as an educational tool to foster interest in atmospheric science.

The project was conceived by students for students and has served as an accessible and welcoming way for student volunteers to learn the basics of project management, research methods, and atmospheric science, all while producing valuable real-world data. The project has provided a jump-start environment for students interested in becoming involved in research early. Each student on the UAH team offered a unique perspective and skill set. Team members contributed skills in data visualization, model evaluation, and automation of tasks though programming. Students familiar with data processing created methods to analyze and store transmitted data. Engineering students soldered and prepped payloads that needed to endure many months of flight. Atmospheric science students learned how to compute trajectories from the wind fields of several numerical weather prediction (NWP) models utilizing the Hybrid Single-Particle Lagrangian Integrated Trajectory (HYSPLIT) model from NOAA's Air Resources Laboratory (ARL). They reached out to scientists at ARL for assistance in learning how to efficiently run the model for many trajectories and to help understand how the data could be used in model evaluation.

Through website design and social media, our team created a way to connect with others while being safe during the COVID-19 pandemic. A custom tracking website (ashballoon.info) we built allowed anyone with internet access to follow the progress of our balloons around the world and leave comments. We embedded the website link into the data packets broadcast by the balloons so people receiving and monitoring our balloon data could learn more about our project. Figure 2 shows some of the comments left on our website during balloon flights. After launching the balloons, we were amazed to see that people from all around the world were inspired by the work we were doing. People from the United States, Germany, Russia, the Netherlands, France, the United Kingdom, and many other countries followed the progress of our balloons. In addition, we found that other hobbyists, teachers, and balloonists were using our flights as educational tools, teaching younger students the benefits of pursuing a STEM project and career path. We are proud to be able to say we inspired others on a global level and we will continue to do so as we pursue future flights.

Fig. 1. Some members of the UAH team at a team-bonding weather balloon recovery mission.

Brought to you by NOAA Central Library | Unauthenticated | Downloaded 07/19/23 04:33 PM UTC

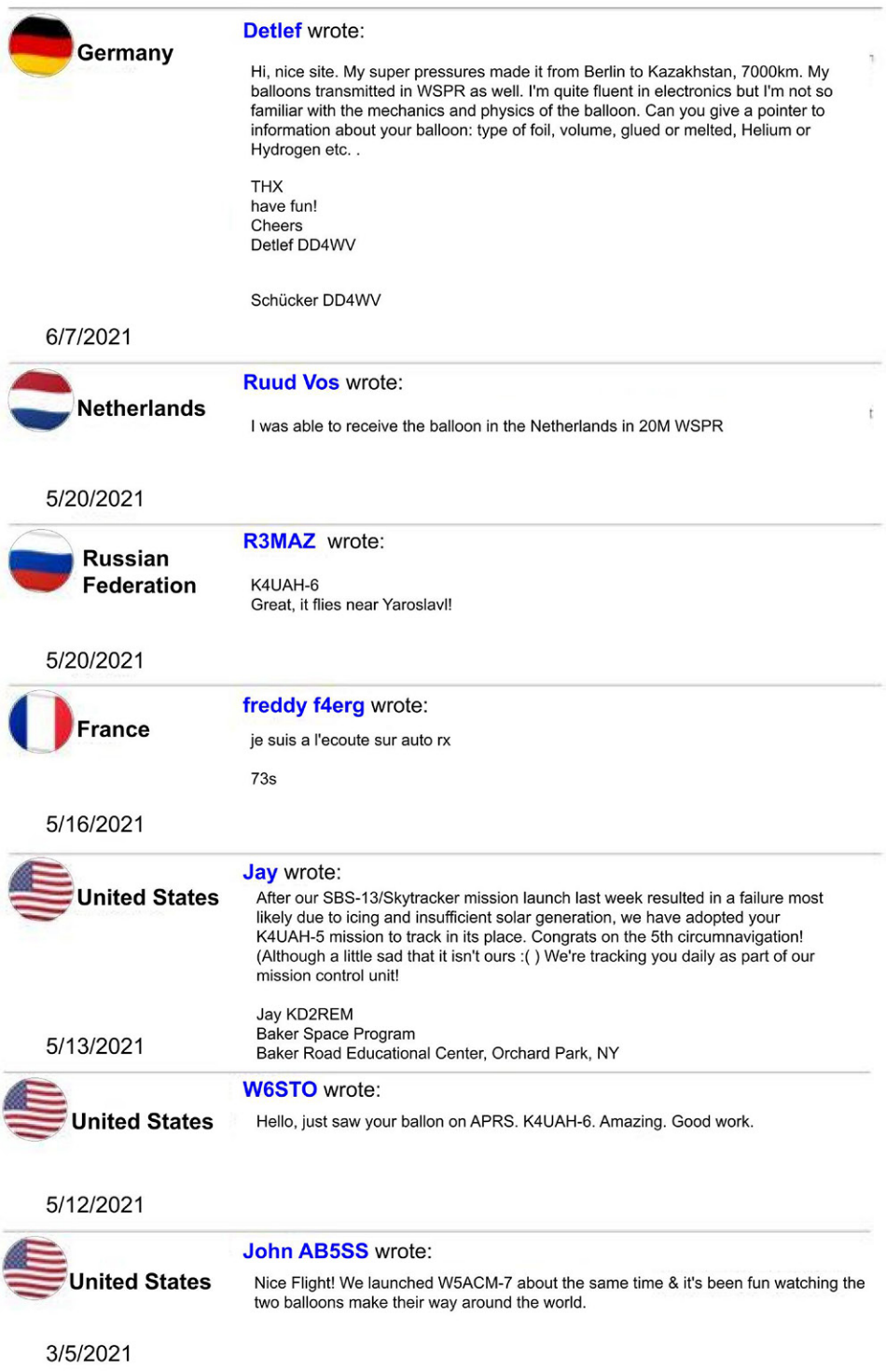

Fig. 2. Some of the comments left on the custom ashballoon.info comment page. STEM groups, ham radio operators, and students show engagement with the balloons.

The balloons

The type of balloon used on this project was a Scientific Balloon Solutions SBS-13 (shown in Fig. 3). This superpressure balloon is very small with dimensions 2.28 m × 0.91 m. The SBS-13 floats at a constant isobaric level of 150 hPa, which varies between about 12 and 14 km MSL.

To sustain a constant altitude, hydrogen is utilized as a lifting gas. Hydrogen allows for longer flights than helium due to its smaller diffusion coefficient. In addition, hydrogen has a higher lift factor (buoyancy), which allows the balloon to fly higher to avoid more severe storms

Brought to you by NOAA Central Library | Unauthenticated | Downloaded 07/19/23 04:33 PM UTC

that produce high-level anvil clouds. Once filled with hydrogen, the SBS-13 is heat sealed, ensuring minimal gas leakage during flights. Five balloons were launched in the phase of the work being reported here. Two of the balloons went down shortly after deployment and did not achieve superpressure level. We found that to ensure a safe transition from ascent to float altitude, these balloons should ideally be launched with clear skies, low winds, and in the early morning to avoid afternoon thermal heating, which can make the balloons ascend too rapidly. Eventually a micro superpressure balloon starts leaking gas and will descend to the ground. These leaks can occur if the balloon encounters unusually strong wind shear and/or tropical convection events. Deflated balloons can be recovered but most end up descending over oceans, making them unrecoverable.

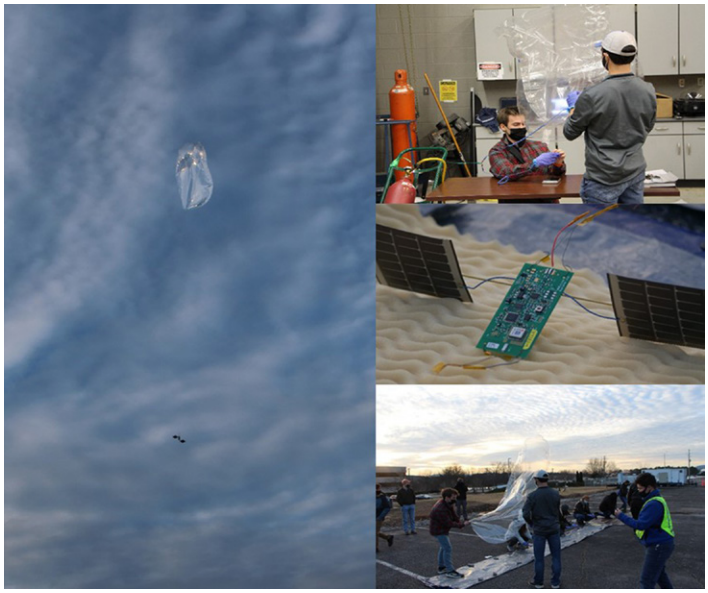

Fig. 3. (left) Superpressure balloon with SkyTracker just after launch. (top right) Members Todd McKinney and Nick Perlaky measuring lift of balloon on a gram scale. (middle right) SkyTracker payload with two 4.8-V solar panels on either side. (bottom right) Paula Tucker (yellow vest) and fellow team members prepare to launch the first balloon.

To track balloon positions, Weak Signal Propagation Reporter (WSPR) is utilized. The WSPR network is a "group of amateur radio operators using a digital mode to probe radio frequency propagation conditions using very low-power transmissions" (Taylor 2022). On every continent, licensed amateur radio operators maintain stations that transmit and listen for WSPR frequencies. Depending on the wavelength of the signal, the distance traveled, and the time the signal was received, the current propagative nature of the ionosphere can be defined (Taylor 2022). The data collected by these stations are uploaded to a public database on the website WSPR.org. This study took advantage of this amateur radio infrastructure by flying a WSPR SkyTracker payload (also shown in Fig. 3) custom build by Bill Brown (wb8elk.com). The SkyTracker is a daytime-only solar-powered transmitter that operates on the 20-m (≈14.09 MHz) WSPR band. The ability of 20-m radiation to propagate off the ionosphere allows the tracker to be heard on an intercontinental scale. See Fig. 4 for a map showcasing the impressive range of a WSPR transmission for one of the days over North Africa. Using WSPR to collect balloon data allows any computer with internet access to view the progress of these balloon flights. To access these data, a custom-written script pulls the data from WSPR.net and uploads them to another amateur radio website called APRS.fi. APRS.fi plots trajectories on a map and allows for downloading position report data in CSV format. The SkyTracker is powered by two PowerFilm 3.6-V solar panels. With solar panels, the SkyTracker weighs approximately 14.50 g with two 10-m antennas suspended up and down from the tracker. Because it is strictly solar powered, the tracker only transmits during the daytime. When powered, the SkyTracker provides a position report every 10 min. The location provided from a WSPR position report is given in a 3.2 km × 4.8 km grid, with the GPS point given for the center of the grid square. From these GPS coordinates, velocity can be calculated based on time between packets. Voltage output is transmitted to monitor tracker health and to view when the system is powering up or powering down for the day. A board temperature sensor

Brought to you by NOAA Central Library | Unauthenticated | Downloaded 07/19/23 04:33 PM UTC

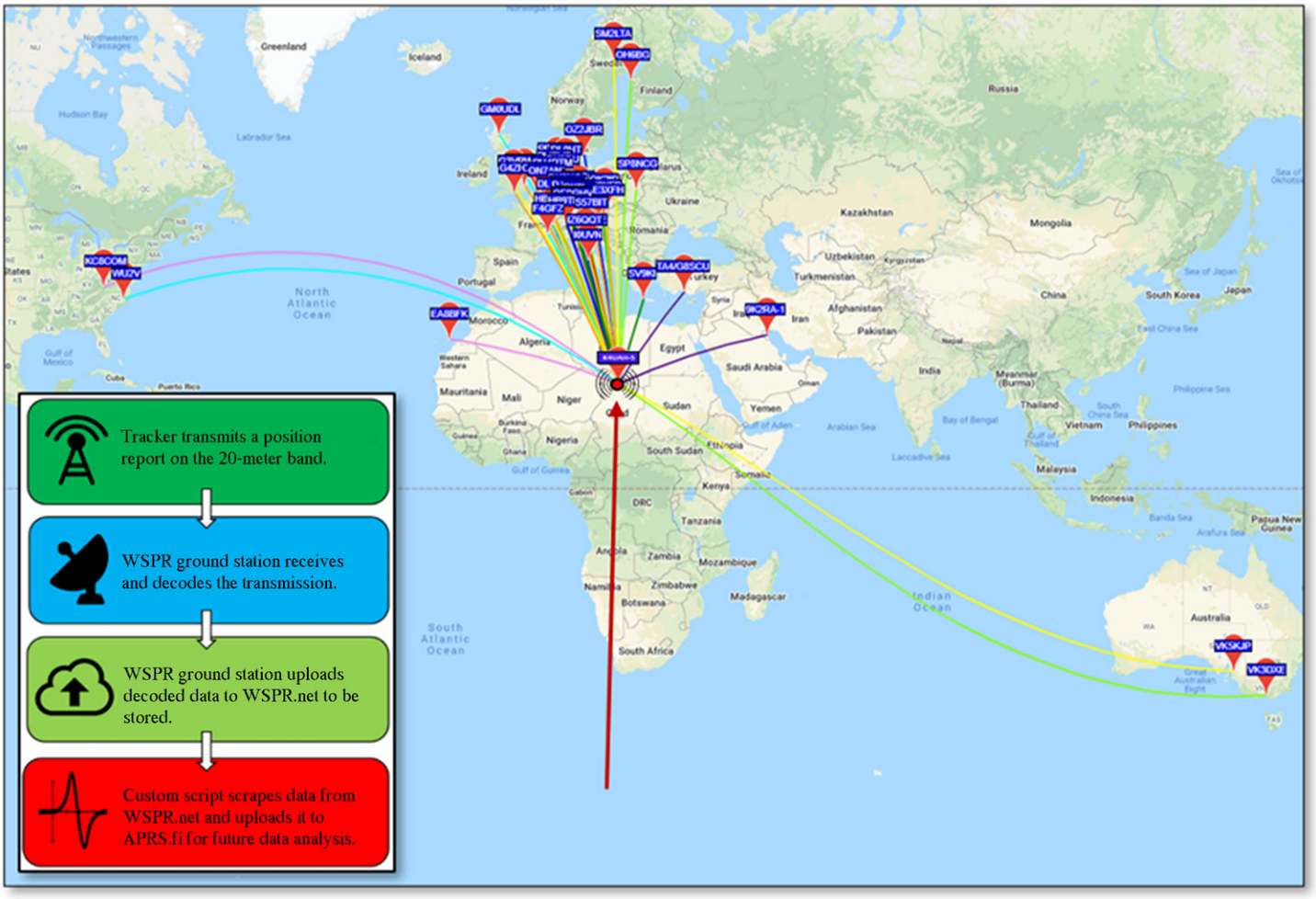

Fig. 4. WSPR map of stations, shown by purple callsign labels, receiving K4UAH-5 transmissions over northern Africa, and a flowchart detailing the data collection process. Red arrow and dot notate balloon position on 27 May 2021. The tracker successfully made contacts with stations in Australia, the Middle East, Europe, the Canary Islands, and the United States, all in the same day.

is included on the tracker, but the temperature measurement not beneficial as it is inflated due to absorption of solar radiation. An example APRS.fi converted packet is shown below:

28.6457°N 15.2915°E
2021–03–28 10:56:18z–2021–03–28 10:56:48z
144 km h^{-1} 89° alt 13420 m
Jufra District, Libya
Solar: 3.600 Volts, Temp: 10 Deg.C, Sats: 12, Lock: 1
7 Sats 4.40 V 13420 m 15C JL78PP QS7LPP KN4TPG WSPR Balloon

The balloons flew under the Federal Aviation Administration's Part 101, which includes "moored balloons, kites, amateur rockets, and unmanned free balloons" (Federal Aviation Administration 2021). These regulations explain weight limits and surface area guidelines for balloon flights. All FAA rules and regulations were followed in this study. Our balloons are so small and light there are essentially no restrictions on where they can fly. The WSPR transmitters also followed all Federal Communications Commission regulations. All transmissions were under call signs of licensed amateur radio operators and WSPR transmitters were programmed to turn off over restricted areas, such as North Korea, Yemen, and the United Kingdom.

Brought to you by NOAA Central Library | Unauthenticated | Downloaded 07/19/23 04:33 PM UTC

There have been many studies utilizing data from balloons on the order of 10–15 m in diameter with float altitudes around 18–20 km, which have flight times on the order of weeks to months, which is similar to ours (Hertzog et al. 2004; Knudsen et al. 2006; Friedrich et al. 2017; Dharmalingam et al. 2019; Conway et al. 2019; Podglajen et al. 2020). These balloons can carry a heavier payload but are significantly larger, more expensive, and difficult to launch than the ones we utilize. In some cases, flights have to be terminated due to flight restrictions (Hertzog et al. 2004). Our balloons have a lower float altitude and thus sample a different part of the atmosphere, providing a complementary dataset to the larger balloons. Notably several studies have repurposed data from Project Loon balloons (https://loon.co) which were intended to help provide internet access to remote areas and not for creation of a scientific dataset (Conway et al. 2019; Friedrich et al. 2017). We show here that data from these micro superpressure balloons which have primarily been used for entertainment and education can similarly be repurposed into a useful scientific dataset.

Description of flight paths and data. The data discussed in this paper were collected between 29 January and 6 August 2021. The balloon trajectories are shown in Fig. 5 while the data collected are shown in Fig. 6. The three balloon missions are identified by call signs K4UAH-4, K4UAH-5, and K4UAH-6. The K4UAH-4 balloon was deployed on 29 January 2021. K4UAH-4 successfully made two complete circumnavigations and generally stayed between latitudes 30° and 45°N, only making drastic shifts in latitude for a trip through Germany and to Alaska. This balloon on average traveled the fastest, sticking to prevalent winter jets at altitudes between 12 and 13 km. The fastest speed of 87 m s^{-1} was recorded over South Korea by the K4UAH-4 balloon. K4UAH-4 remained in flight for 32 days until encountering strong wind shear off the coast of California, where it went down on 2 March 2021. K4UAH-5 was the second balloon launched and was deployed on 20 February 2021. K4UAH-5 remained in the air for 106 days and successfully made six circumnavigations covering an altitude range of 13–14 km. K4UAH-5 traveled to more southern locations, where it made multiple passes over Africa. It also made a rare trip to the equator, where it missed the zero-latitude line by 1° over the Pacific Ocean. K4UAH-5 on average took longer to circumnavigate due to flying in the lower-wind-speed conditions of low latitudes. After encountering a large tropical storm off the coast of Florida, the K4UAH-5 balloon went down over the North Atlantic Ocean. The final balloon, K4UAH-6, was deployed on 8 March 2021, and holds our current record for flight time, flying for 151 days and making eight total circumnavigations. K4UAH-6 was the only flight to travel into the Arctic Circle and had the most drastic shifts in latitude, often traveling with little to no zonal flow. Because the K4UAH-6 balloon remained in Arctic flow patterns for the later part of its flight, it was able to avoid more extreme tropical storms. Only after traveling over an extreme wind gradient off the coast of Nova Scotia did the balloon finally leak and come down over the North Atlantic Ocean.

The unique nature of each balloon path has allowed for data analysis in different flow patterns. The data collected from all balloons ranged between latitudes 1.4° and 81.0°N at altitudes of 12 and 14 km with a sample size of over 10,000 data points. Because all launch dates were in late winter in the Northern Hemisphere, balloons were often entrained into polar jets. The most common jet locations were over eastern China, the northwestern United States, and off the coast Nova Scotia. These jets had velocities between 150 and 316 km h^{-1}. As the season in the Northern Hemisphere moved from winter to spring, average balloon velocities were found to decrease. In the summer seasons, zonal flow velocities decreased rapidly over the course of July as balloon trajectories were influenced more by synoptic-level pressure cells rather than global jet patterns. Almost every circumnavigation included a trip through a narrow latitude range over the Himalayas. This area, which extends from western

Brought to you by NOAA Central Library | Unauthenticated | Downloaded 07/19/23 04:33 PM UTC

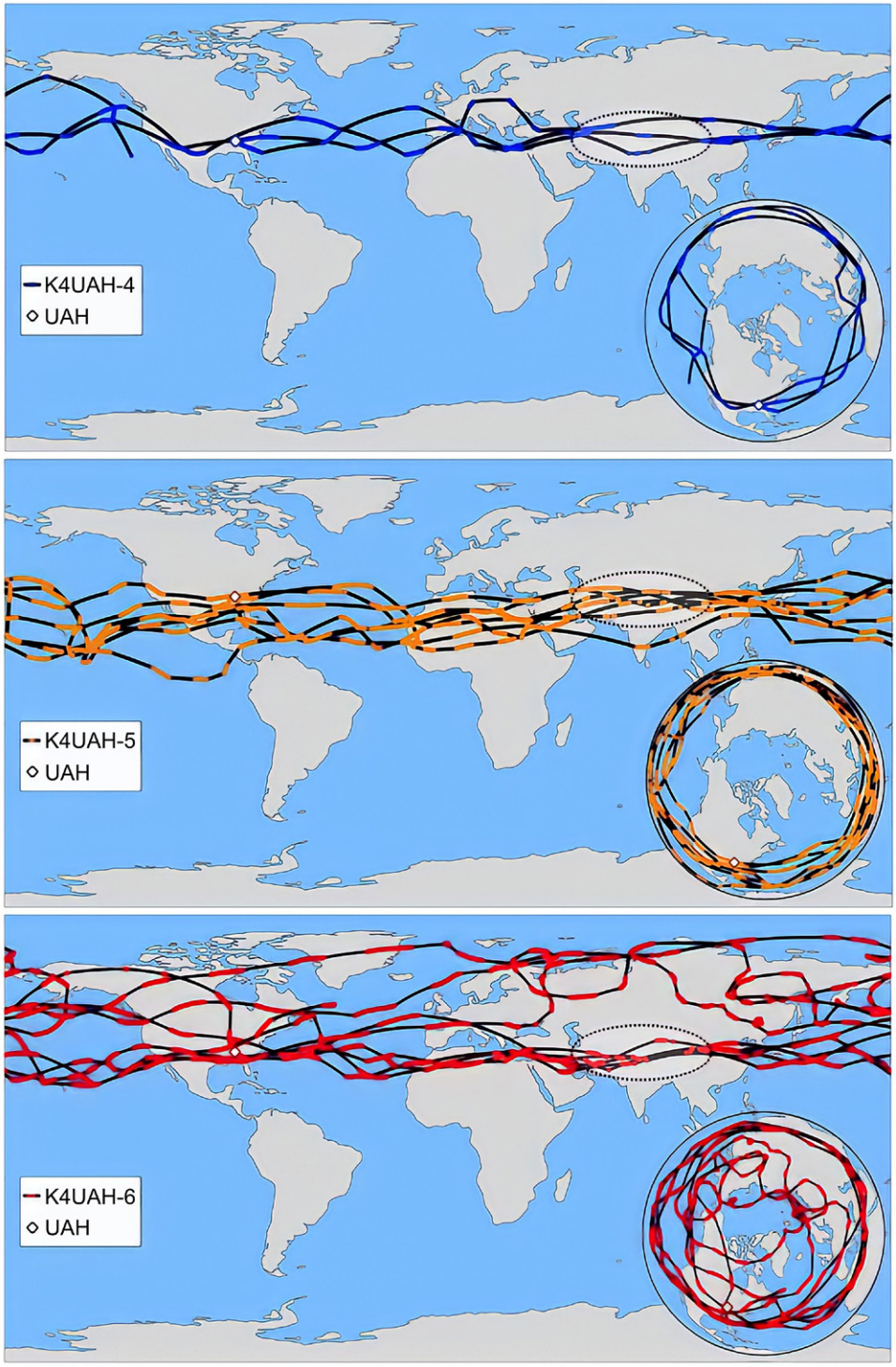

Fig. 5. Maps displaying balloon trajectories. White diamond represents launch location at Severe Weather Institute–Radar and Lightning Laboratories at University of Alabama at Huntsville (UAH). Colored lines represent times when the balloon was awake and transmitting data. Straight black lines represent times of no data. The Himalayan corridor is notated with a dotted oval.

Tibet to central China, is circled in Fig. 5 and we refer to it as the Himalayan corridor. Only K4UAH-6's trip to the Arctic and K4UAH-5's trip through southern India avoided this area.

Methods

Atmospheric transport and dispersion model. Atmospheric transport and dispersion models (ATDM) are widely used in conjunction with NWP models to predict or diagnose the transport of materials in the atmosphere. These include dust (Creamean et al. 2013),

Brought to you by NOAA Central Library | Unauthenticated | Downloaded 07/19/23 04:33 PM UTC

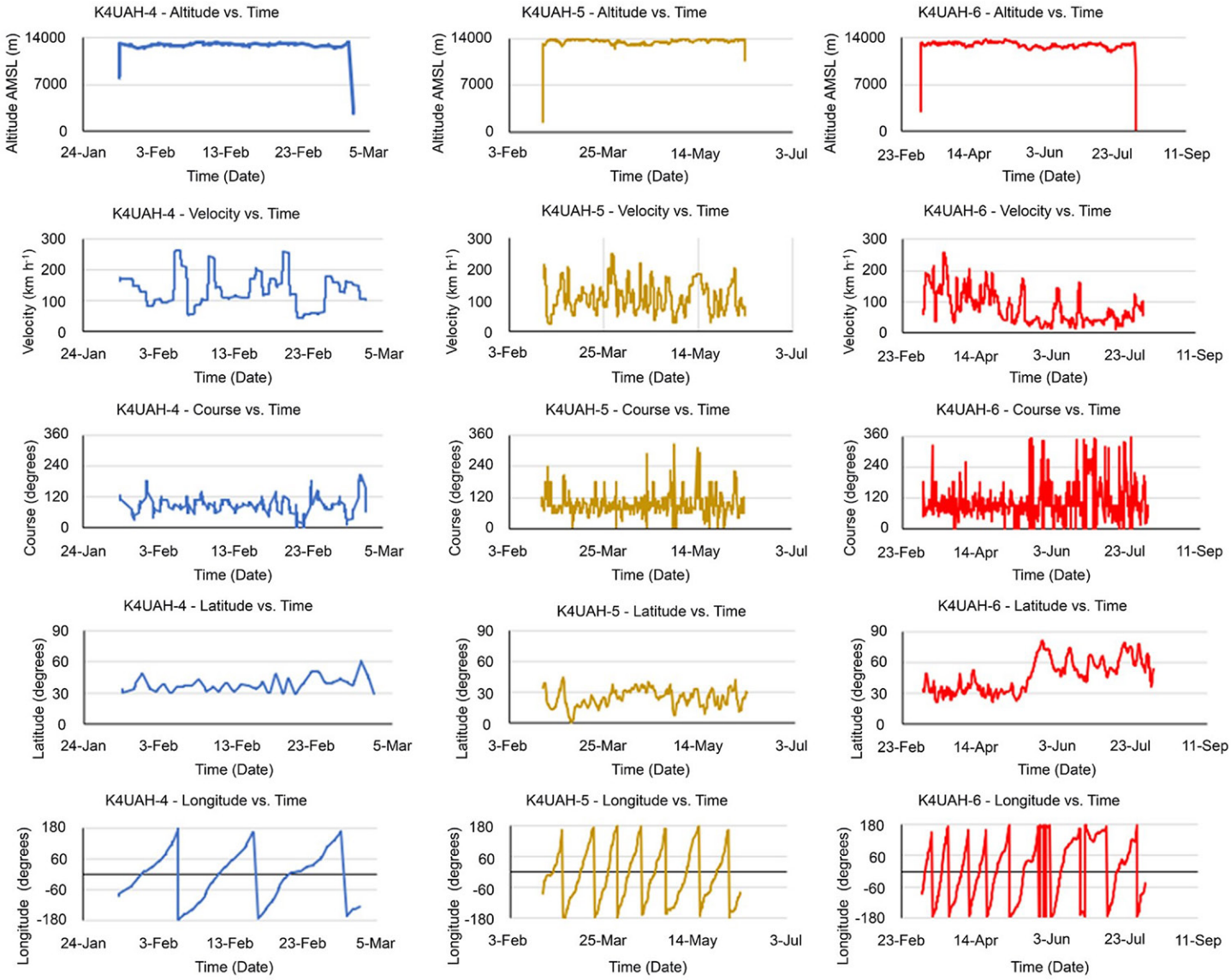

Fig. 6. Graphs of all K4UAH balloon data over each flight. Times are given in date format.

volcanic emissions (Zuev et al. 2017), smoke from fires (Fromm et al. 2010), halogenated very short-lived substances (Tzella and Legras 2011), microplastics (González-Pleiter et al. 2021), and even microorganisms (Smith et al. 2018). Trajectories have also been used to study cloud formation (Ueyama et al. 2018). Consequently, the accuracy of airmass trajectories is of much interest (Stohl and Koffi 1998). Here we present a relatively simple but informative analysis of trajectory error for several different NWP models.

We utilize the HYSPLIT model developed and maintained at NOAA ARL (Stein et al. 2015). HYSPLIT can simulate both simple airmass trajectories and more complex dispersion, deposition, and chemical transformation processes. HYSPLIT's trajectory modality was utilized in this work, in which air parcel paths are calculated from the wind field provided by an NWP model. The advection of a particle is given by Draxler and Hess (1998):

$$P'(t+\Delta t) = P(t) + V(P,t)\Delta t, \tag{1}$$

where $P'(t+\Delta t)$ is the initial position calculated from average of the three-dimensional velocity vector, with the final position given by

$$P(t+\Delta t) = P(t) + 0.5[V(P,t) + V(P',t+\Delta t)]\Delta t. \tag{2}$$

Brought to you by NOAA Central Library | Unauthenticated | Downloaded 07/19/23 04:33 PM UTC

The accuracy of a HYSPLIT-calculated trajectory mainly reflects the accuracy of the modeled wind fields from the NWP model as well as uncertainties introduced by characterization of subgrid flow variations through interpolation (Draxler and Hess 1998).

Meteorological models. By comparing different NWP models and their spatial resolutions, we can understand what models perform the best in certain global conditions. Trajectories were calculated using output from the National Centers for Environmental Information's (NCEP) Global Forecasting System (GFS), Global Data Assimilation System (GDAS), and the Global Ensemble Forecast System (GEFS). The GFS has 0.25°, 0.5°, or 1° spatial resolution, 3-h temporal resolution, and 41 vertical levels. GEFS has 31 members with 0.50° spatial resolution, 3-h temporal resolution, and 20 vertical levels (National Centers for Environmental Information 2022). The GEFS quantifies uncertainties by generating multiple forecasts that produce a range of outcomes based on different simulation configurations in the generation of modeled meteorological results. The GEFS has a "control" and "average" forecast among the members. The "control" is the model's best guess of the current meteorological conditions, while the "average" combines the differences applied to the other members into one synthesized forecast. GFS and GEFS forecasts are produced every 6 h at 0000, 0600, 1200, and 1800 UTC. Each forecast is for 360 h in the future; GDAS is an analysis dataset, produced after the fact using measurements to create an estimate of past atmospheric conditions.

Trajectory error analysis. Superpressure balloon trajectories have been utilized to analyze winds in the stratosphere (Conway et al. 2019) evaluate wind fields from NWP models (Friedrich et al. 2017, and references therein). They have also been used to study the effect of gravity waves in the lower stratosphere and their representation in NWP models (Podglajen et al. 2016, 2020). Here we present a relatively simple but informative analysis of trajectory error that can be used to compare the different meteorological models described above.

To characterize the error of modeled trajectories, the absolute horizontal transport deviation, AHTD, and relative horizontal transport deviation, RHTD, were used (Stohl and Koffi 1998):

$$\mathrm{AHTD}(t) = \sqrt{[X(t)-x(t)]^2+[Y(t)-y(t)]^2}, \tag{3}$$

$$\mathrm{RHTD}(t) = \frac{\mathrm{AHTD}(t)}{L}, \tag{4}$$

where (X, Y) are locations of the superpressure balloon and (x, y) are the locations of the calculated trajectories. The AHTD is simply the distance between the balloon position and the calculated trajectory position at time t. It is common in the literature to report AHTD for a certain amount of time. For instance Friedrich et al. (2017) report mean 5-day trajectory separation of 621 km for trajectories generated with the Modern-Era Retrospective Analysis for Research and Applications 2 (MERRA-2) wind fields.

The AHTD is zero at $t = 0$, with the trajectory and the balloon position starting at the same point. Here we take L to be the length of the modeled trajectory because data for the observed trajectory are not available during nighttime.

Trajectory forecasts were started at the time the balloon started sending information each day using the closest preceding forecast cycle (e.g., if the balloon started sending information at 0800 UTC, the forecast produced at 0600 UTC would be utilized).

Brought to you by NOAA Central Library | Unauthenticated | Downloaded 07/19/23 04:33 PM UTC

Results and discussion

First, we look at AHTD and RHTD for short trajectory forecasts of duration up to 6 h. We then show some qualitative results for long trajectory forecasts of up to 360 h, the full length of the forecast data available from the NWP model. Finally we study some trajectories in areas that have unique synoptic level conditions. These include areas with high elevations and stronger low pressure–dominated flow.

Short forecasts. For short forecast time periods (less than 6 h) we found that AHTD values have a linear relationship to forecast time and an average rate of separation, AHTD/t, can be determined from a fit to the data (see Fig. 6). The higher resolution GFS 0.25° had the smallest average rate of separation of 15 km h^{-1}. The GFS 1.0°, GFS 0.5°, and GDAS 1.0° all had an average rate of separation of 17 km h^{-1}. The half-degree improvement in resolution from a 1.0° to a 0.5° weather model did not improve the accuracy of simulated trajectories up to 6 h. Also, there was no apparent difference in RHTD or AHTD between the GDAS and GFS, which is of interest because the GDAS ingests more observations than the GFS (National Center for Atmospheric Research 2015) and trajectories calculated from an analysis dataset are sometimes used for evaluation of trajectories calculated from a forecast (Stunder 1996).

The RHTD is used to compare trajectory accuracy under a variety of global conditions. The comparison of RHTD versus balloon velocity is an indication of the accuracy of the calculated trajectory in relation to the horizontal motion of the atmosphere. When AHTD is proportional to time, the RHTD is expected to be inversely proportional to velocity. This trend can be seen in Fig. 7. There is a large amount of scatter in the RHTD versus velocity as well as AHTD versus time plots indicating that other factors are important in determining trajectory error. For instance, we noticed that RHTD values tend to be higher in remote areas such as oceans where meteorological data from soundings are not available. This connection to lack of meteorological data such as soundings will be examined in more depth in future work.

Long-range forecasts. Long-range forecasts, up to 360 h, were performed using the GFS 0.25°. At long forecast times, the relationship between AHTD and time becomes more complex. Mean AHTD values were found to be 1500 ± 1000 km after 5 days and 2700 ± 2000 km after 10 days. The average trajectory separations as well as the standard deviations are somewhat larger than were found in other studies (Hertzog et al. 2004; Knudsen et al. 2006; Boccara et al. 2008; Friedrich et al. 2017). The lower float altitude probably contributes as our balloons are exposed to more chaotic synoptic flow patterns. Areas of strong velocity changes, such as when the balloons entered and exited upper-level jets, could have contributed to these variations in AHTD. Also most of these studies utilized an analysis rather than a forecast, which would be expected to be more accurate.

In long-range forecasts AHTD and RHTD values did not always increase with time. Values could decrease in some cases such as when balloons encountered an area where the flow was converging. A recurring feature was AHTD and RHTD values increased after passing through the Himalayan corridor. An example is shown in Fig. 8, where a long duration simulation for a flight that passed through the Himalayan corridor is compared to one that instead traveled through southern India. For the flight through southern India, error values were the lowest calculated from the dataset. RHTD values for the GFS 0.25° were generally below 10% for the whole 362-h forecast. For balloons that traveled through the Himalaya corridor, RHTD values commonly increased to 50%. Figure 8 also displays balloon and model velocity versus forecast time. The transition from slower to faster wind speeds was misrepresented by the model when entering the Himalayan corridor. Upon approaching this area, the simulated balloon track fell behind the real balloon track causing RHTD to increase sharply after forecast hour 100. However, the simulated balloon experienced an increase in speed about the same time

Brought to you by NOAA Central Library | Unauthenticated | Downloaded 07/19/23 04:33 PM UTC

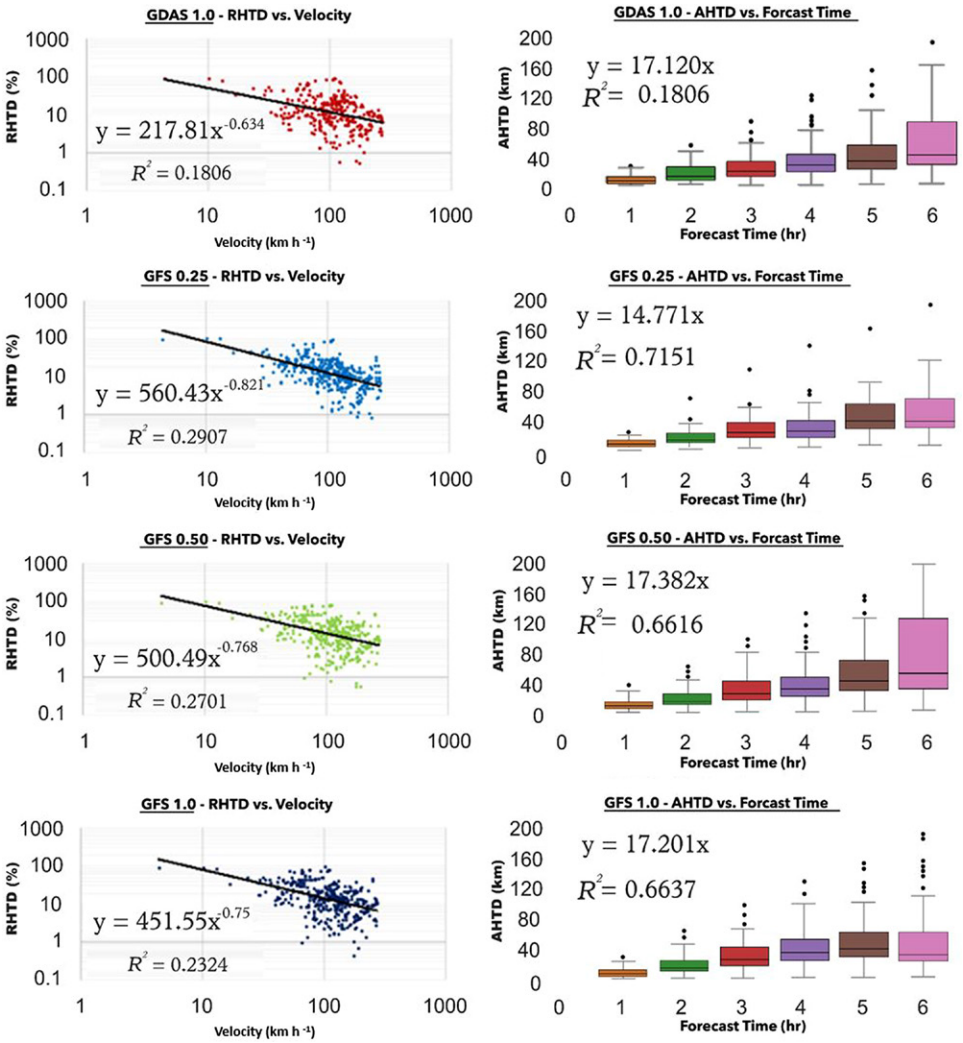

Fig. 7. (left) RHTD and (right) AHTD results for 6-h forecasts of the (from top to bottom) GDAS 1.0°, GFS 0.25°, GFS 0.5°, and GFS 1.0°.

the real balloon started slowing down and thus significantly caught up to the real balloon by forecast hour 200. The simulated trajectory followed the path of the balloon quite well, but was offset in time, which caused the RHTD to oscillate. When the 362-h run concluded, the final predicted balloon position for the flight that went through the Himalaya corridor was off by the whole North American continent compared to actual balloon position. More meteorological data and a better representation of terrain and surface to atmosphere interactions might improve this type of forecast.

Ensemble forecast. Although trajectory forecasts may be improved, some uncertainty will always remain. An ensemble of trajectories can be utilized to capture this inherent uncertainty. To create the ensemble, HYSPLIT is driven with each member of the GEFS. In slow-moving air masses and areas of dominant synoptic level pressure cells, GEFS trajectory ensembles can show significant spread. Figure 9 shows a case in which the K4UAH-6 balloon was caught in a large low pressure system over the North Pacific Ocean. HYSPLIT GEFS trajectories were initialized in the entrance region of a low pressure cell at 1800 UTC 23 June 2021, at coordinates 41.729°N, 167.958°W, and at an altitude of 12,700 m MSL. In this case, the K4UAH-6 balloon was caught in a large low pressure system over the North Pacific Ocean. As the balloon wrapped around the cell and its direction of movement trended northward, the HYSPLIT trajectories demonstrated high skill, where all RHTD values remained below 15%. After 42 h, the balloon was positioned east of the low pressure and

Brought to you by NOAA Central Library | Unauthenticated | Downloaded 07/19/23 04:33 PM UTC

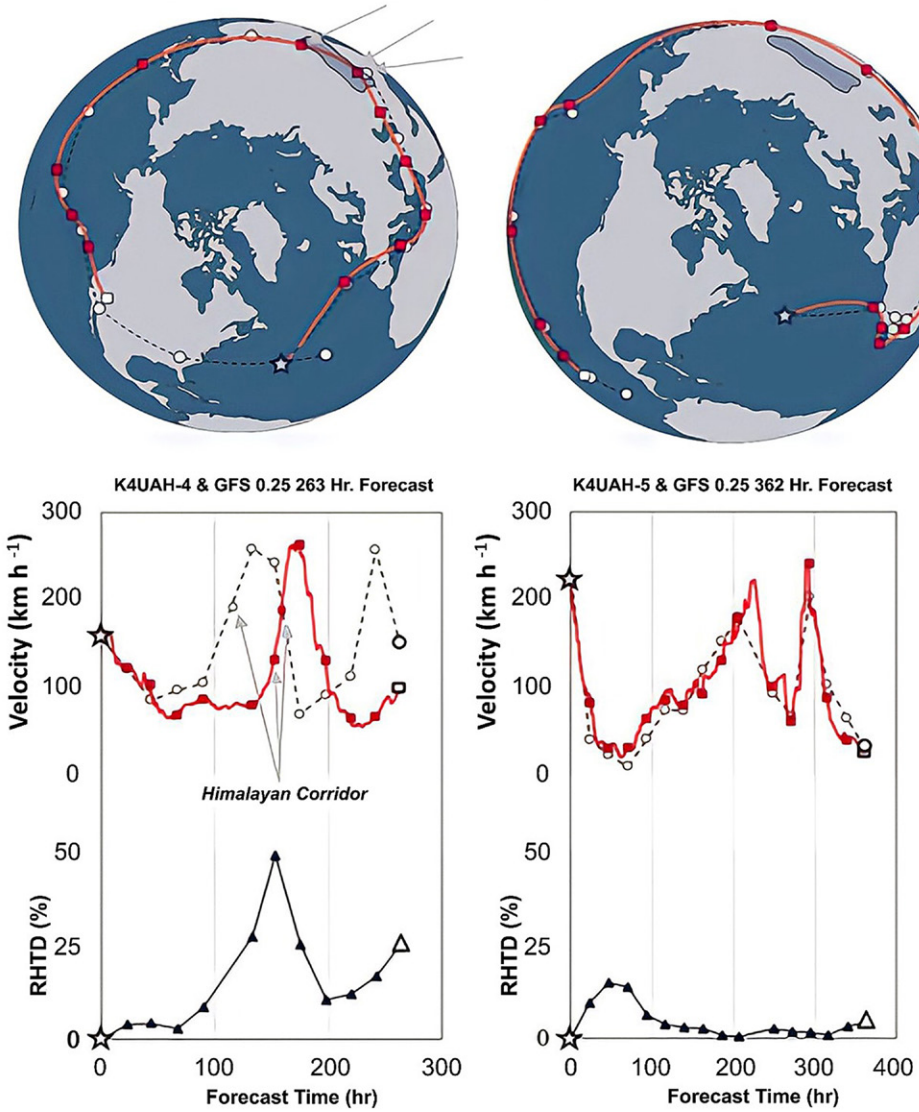

Fig. 8. Comparison of long-range, 360-h, forecast with the GFS 0.25° model for (left) a balloon entering the Himalayan corridor vs (right) a balloon dodging it. Velocity and RHTD vs forecast hour are plotted, with circles with dotted lines denoting observed balloon values, and red squares with red lines denoting calculated HYSPLIT values. Arrows indicate when the model and balloon where inside the Himalayan corridor. White stars denote the model start point, and white shapes denote the end of model analysis. The Himalayan corridor is shown by a faded blue shape overlaid on the maps.

reached the point of maximum meridional movement and very low zonal velocity. At this point, the paths from the ensemble members began diverging and RHTD values increased rapidly over time for most members. The majority of trajectories eventually exited the pressure cell north of Alaska. Two exited the cell closer to the actual path of the balloon. Some trajectories remained in the area of low pressure to the end of the forecast. Ultimately, ensemble trajectories demonstrated high skill when entering a low pressure system but had lower skill predicting movement as the flow exited the cell. The next step will be to develop and apply measures of how well the trajectory ensemble captures uncertainty.

Conclusions and future work.

We have shown that data from micro superpressure balloon payloads can be a valuable scientific dataset. For short forecast times, we find a linear relationship between AHTD and time and define a mean separation rate for modeled versus observed trajectories. We find the GFS 0.25° has the smallest separation rate of the models we analyzed. We have also demonstrated

Brought to you by NOAA Central Library | Unauthenticated | Downloaded 07/19/23 04:33 PM UTC

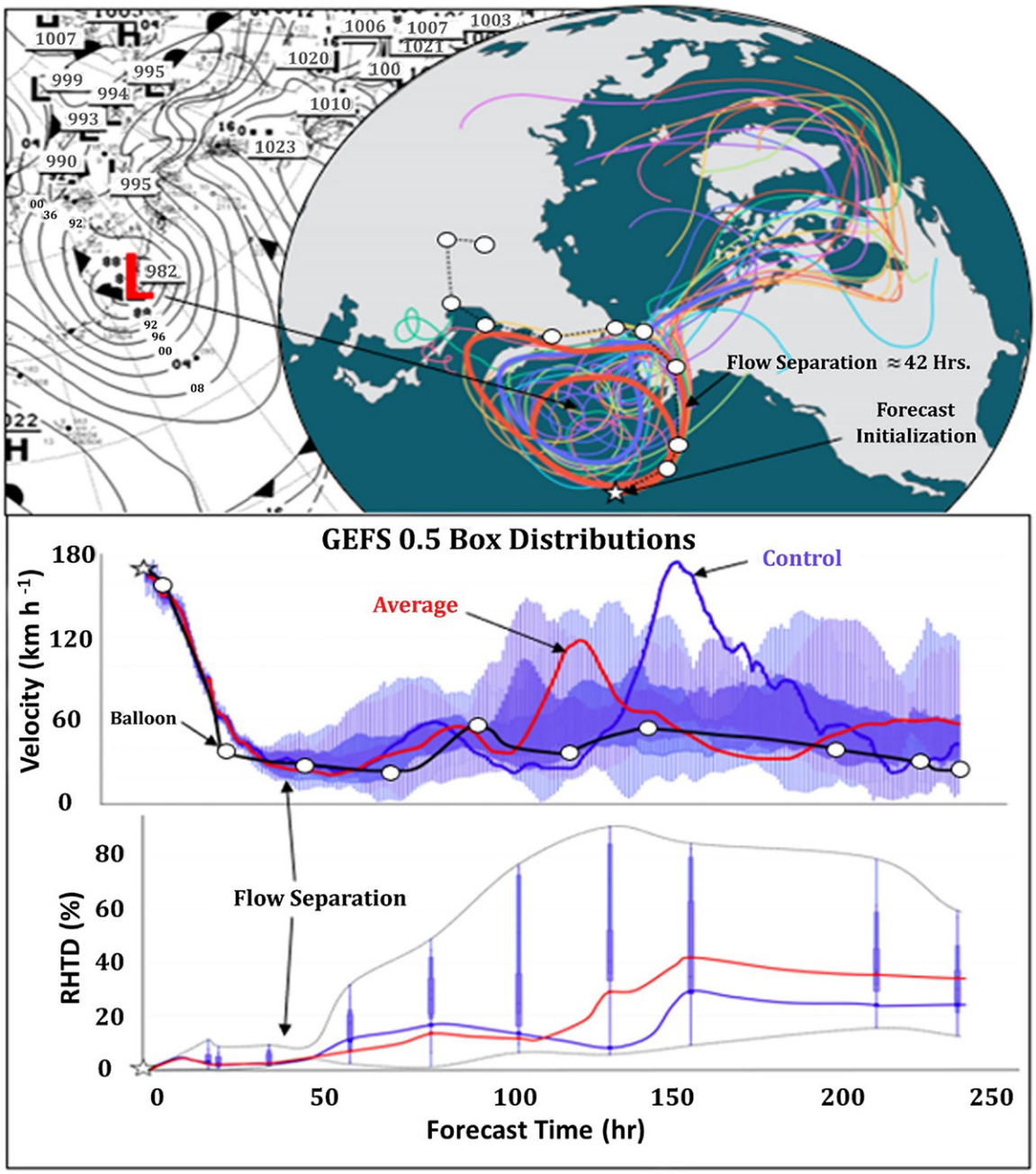

Fig. 9. K4UAH-6 balloon entering and exiting a low pressure system with GEFS ensemble member analysis. (top left) The synoptic pressure conditions of the area. (top right) Balloon trajectories and ensemble trajectories, with the average GEFS plotted in red, the control GEFS plotted in blue, the balloon indicated by circles with dotted lines, and multiple-colored lines showing all other 30 ensemble members. The separation of ensemble members occurs around 42 h into the forecast. (middle) A 1-h time-step velocity vs forecast time of all members is shown in a box distribution with the members that left the pressure cell plotted in darker blue. (bottom) Resulting distribution of RHTD values; the time interval is roughly 24 h. Due to the lack of transmissions during night, there are uneven gaps in the box distribution plot.

the influence of the Himalayan Mountain range (aka the Himalayan corridor) and strong synoptic-level gradients (low pressure systems) on predicting airmass transport. Both were shown to greatly lower the skill of trajectory forecasts.

Groups around the world continue to deploy micro superpressure balloons for fun and education purposes. We are exploring if it is feasible to collect, archive, and utilize data from balloons launched by other groups and individuals, which are often discarded. For any students, ham radio operators, or other STEM groups who are interested in deploying these

Brought to you by NOAA Central Library | Unauthenticated | Downloaded 07/19/23 04:33 PM UTC

balloons, it is important to meet a few criteria to make these flights useful for meteorological studies. First, it is important that balloon location data are at least at a 3.2 km × 4.8 km resolution. Anything higher is too coarse of a resolution to pair with NWP trajectories. In addition, groups are encouraged to transmit data at a standard 10-min interval to provide as much data as possible during the solar day. Finally, balloon data should be uploaded to a public data source, such as APRS.fi, to allow for easy access for researchers wanting to utilize the data for model studies. Other datasets of Lagrangian balloon trajectories have been used repeatedly (Friedrich et al. 2017; Conway et al. 2019; Dharmalingam et al. 2019). If micro superpressure balloon data are publicly available, there is an expectation that students and researchers will utilize the datasets far into the future.

It is possible that these balloons could one day be launched by meteorologists alongside weather balloons at sounding stations to provide meteorological data for models (Keil 2004; Manobianco et al. 2008a). Projects like this will help pave the way for such a capability (Manobianco et al. 2008b). As a student-driven team, we will continue to launch balloons to learn more about the incredible planet on which we live.

Acknowledgments. This student project would not have been possible without the support of Dr. Alice Crawford and Dr. Mark Cohen from NOAA's Air Resource Laboratory. The authors gratefully acknowledge the NOAA Air Resources Laboratory (ARL) for the provision of the HYSPLIT transport and dispersion model and READY website (www.ready.noaa.gov) used in the publication. Bill Brown's (WB8ELK) experience with amateur radio and high-altitude balloons has made the balloon flights possible. A big thank you to Dr. Michael Newchurch and Dr. Kevin Knupp for their mentorship and advice and allowing the UAH team to launch at Severe Weather Institute–Radar and Lighting Laboratories. Paula Tucker's OSHA safety knowledge provided the UAH team with a safe launch environment when working with hydrogen. The funding and support of the Space Hardware Club at UAH and the Alabama Space Grant Consortium allowed these balloon flights to be possible.

Data availability statement. All balloon data were collected through the public websites WSPR.net and APRS.fi. These data are freely available to the public. The authors greatly appreciate the resources that WSPR.net and APRS.fi provides to the ham radio community.

Brought to you by NOAA Central Library | Unauthenticated | Downloaded 07/19/23 04:33 PM UTC

References

Boccara, G., A. Hertzog, C. Basdevant, and F. Vial, 2008: Accuracy of NCEP/NCAR reanalyses and ECMWF analyses in the lower stratosphere over Antarctica in 2005. *J. Geophys. Res.*, **113**, D20115, https://doi.org/10.1029/2008JD010116.

Carpi, A., D. M. Ronan, H. M. Falconer, H. H. Boyd, and N. H. Lents, 2013: Development and implementation of targeted stem retention strategies at a Hispanic-serving institution. *J. Hisp. Higher Educ.*, **12**, 280–299, https://doi.org/10.1177/1538192713486279.

Cathey, H. M., 2009: The NASA super pressure balloon—A path to flight. *Adv. Space Res.*, **44**, 23–38, https://doi.org/10.1016/j.asr.2009.02.013.

Conway, J. P., G. E. Bodeker, D. W. Waugh, D. J. Murphy, C. Cameron, and J. Lewis, 2019: Using Project Loon superpressure balloon observations to investigate the inertial peak in the intrinsic wind spectrum in the midlatitude stratosphere. *J. Geophys. Res. Atmos.*, **124**, 8594–8604, https://doi.org/10.1029/2018JD030195.

Creamean, J. M., and Coauthors, 2013: Dust and biological aerosols from the Sahara and Asia influence precipitation in the western U.S. *Science*, **339**, 1572–1578, https://doi.org/10.1126/science.1227279.

Dharmalingam, S., R. Plougonven, A. Hertzog, A. Podglajen, M. Rennie, L. Isaksen, and S. Kebir, 2019: Accuracy of balloon trajectory forecasts in the lower stratosphere. *Atmosphere*, **10**, 102, https://doi.org/10.3390/atmos10020102.

Draxler, R. R., and G. D. Hess, 1998: An overview of the HYYSPLIT_4 modeling system for trajectories, dispersion, and deposition. *Aust. Meteor. Mag.*, **47**, 195–308.

Federal Aviation Administration, 2021: Part 101—Moored balloons, kites, amateur rockets, and unmanned free balloons. Code of Federal Regulations 14, Chapter 1F, accessed 6 August 2021, www.ecfr.gov/current/title-14/chapter-I/subchapter-F/part-101.

Florence, S., N. Bajaj, and G. Chiu, 2018: Inspiring future generations in stem field through robotics competition: A college student mentoring approach. *Mech. Eng.*, **140**, S13–S17, https://doi.org/10.1115/1.2018-MAR-5.

Friedrich, L. S., A. J. McDonald, G. E. Bodeker, K. E. Cooper, J. Lewis, and A. J. Paterson, 2017: A comparison of Loon balloon observations and stratospheric reanalysis products. *Atmos. Chem. Phys.*, **17**, 855–866, https://doi.org/10.5194/acp-17-855-2017.

Fromm, M., D. T. Lindsey, R. Servranckx, G. Yue, T. Trickl, R. Sica, P. Doucet, and S. E. Godin-Beekmann, 2010: The untold story of pyrocumulonimbus. *Bull. Amer. Meteor. Soc.*, **91**, 1193–1210, https://doi.org/10.1175/2010BAMS3004.1.

Gilfort, J., 2017: Bill Brown, WB8ELK: Master of high-altitude balloon projects. *QST*, Newington, CT, 79–80, https://arrl.org/qst/.

González-Pleiter, M., and Coauthors, 2021: Occurrence and transport of microplastics sampled within and above the planetary boundary layer. *Sci. Total Environ.*, **761**, 143213, https://doi.org/10.1016/j.scitotenv.2020.143213.

Hertzog, A., C. Basdevant, F. Vial, and C. R. Mechoso, 2004: The accuracy of stratospheric analyses in the Northern Hemisphere inferred from long-duration balloon flights. *Quart. J. Roy. Meteor. Soc.*, **130**, 607–626, https://doi.org/10.1256/qj.03.76.

Keil, A., 2004: Assimilating data from a simulated global constellation of stratospheric balloons. *Quart. J. Roy. Meteor. Soc.*, **130**, 2475–2493, https://doi.org/10.1256/qj.03.219.

Knudsen, B., T. Christensen, A. Hertzog, A. Deme, F. Vial, and J. P. Pommereau, 2006: Accuracy of analysed temperatures, winds and trajectories in the Southern Hemisphere tropical midlatitude stratosphere as compared to long-duration balloon flights. *Atmos. Chem. Phys.*, **6**, 5391–5397, https://doi.org/10.5194/acp-6-5391-2006.

Manobianco, J., J. G. Dreher, M. L. Adams, M. Buza, R. J. Evans, and J. L. Case, 2008a: How nanotechnology can revolutionize meteorological observing with Lagrangian drifters. *Bull. Amer. Meteor. Soc.*, **89**, 1105–1110, https://doi.org/10.1175/2008BAMS2529.1.

——, ——, R. J. Evans, J. L. Case, and M. L. Adams, 2008b: The impact of simulated super pressure balloon data on regional weather analyses and forecasts. *Meteor. Atmos. Phys.*, **101**, 21–41, https://doi.org/10.1007/s00703-008-0313-8.

National Center for Atmospheric Research, 2015: What's the difference between GFS and FNL? National Center for Atmospheric Research, accessed 5 May 2022, https://ncarrda.blogspot.com/2015/04/whats-difference-between-gfs-and-fnl.html.

National Centers for Environmental Information, 2022: Global Ensemble Forecast System (GEFS). National Centers for Environmental Information, accessed 5 May 2022, www.ncei.noaa.gov/products/weather-climate-models/global-ensemble-forecast.

National Weather Service, 2022: Education corner weather balloon. National Weather Service, accessed 5 May 2022, www.weather.gov/gjt/education_corner_balloon.

Peterman, K., R. Kermish-Allen, G. Knezek, R. Christensen, and T. Tyler-Wood, 2016: Measuring student career interest within the context of technology-enhanced STEM projects: A cross-project comparison study based on the Career Interest Questionnaire. *J. Sci. Educ. Technol.*, **25**, 833–845, https://doi.org/10.1007/s10956-016-9617-5.

Podglajen, A., R. Plougonven, A. Hertzog, and B. Legras, 2016: A modelling case study of a large-scale cirrus in the tropical tropopause layer. *Atmos. Chem. Phys.*, **16**, 3881–3902, https://doi.org/10.5194/acp-16-3881-2016.

——, A. Hertzog, R. Plougonven, and B. Legras B. Legras, 2020: Lagrangian gravity wave spectra in the lower stratosphere of current (re)analyses. *Atmos. Chem. Phys.*, **20**, 9331–9350, https://doi.org/10.5194/acp-20-9331-2020.

Smith, D. J., and Coauthors, 2018: Airborne bacteria in Earth's lower stratosphere resemble taxa detected in the troposphere: Results from a new NASA Aircraft Bioaerosol Collector (ABC). *Front. Microbiol.*, **9**, 1752, https://doi.org/10.3389/fmicb.2018.01752.

Stein, A. F., R. R. Draxler, G. D. Rolph, B. J. B. Stunder, M. D. Cohen, and F. Ngan, 2015: NOAA's HYSPLIT atmospheric transport and dispersion modeling system. *Bull. Amer. Meteor. Soc.*, **96**, 2059–2077, https://doi.org/10.1175/BAMS-D-14-00110.1.

Stohl, A., and N. E. Koffi, 1998: Evaluation of trajectories calculated from ECMWF data against constant volume balloon flights during ETEX. *Atmos. Environ.*, **32**, 4151–4156, https://doi.org/10.1016/S1352-2310(98)00185-X.

Stunder, B. J. B., 1996: An assessment of the quality of forecast trajectories. *J. Appl. Meteor.*, **35**, 1319–1331, https://doi.org/10.1175/1520-0450(1996)035<1319:AAOTQO>2.0.CO;2.

Taylor, J., 2022: Weak Signal Propagation Reporter network (WSPRnet). J. Taylor, accessed 5 May 2022, https://wsprnet.org/drupal/.

Tzella, A., and B. Legras, 2011: A Lagrangian view of convective sources for transport of air across the tropical tropopause layer: Distribution, times and the radiative influence of clouds. *Atmos. Chem. Phys.*, **11**, 12 517–12 534, https://doi.org/10.5194/acp-11-12517-2011.

Ueyama, R., E. J. Jensen, and L. Pfister, 2018: Convective influence on the humidity and clouds in the tropical tropopause layer during boreal summer. *J. Geophys. Res. Atmos.*, **123**, 7576–7593, https://doi.org/10.1029/2018JD028674.

Zuev, V. V., V. D. Burlakov, A. V. Nevzorov, V. L. Pravdin, E. S. Savelieva, and V. V. Gerasimov, 2017: 30-year lidar observations of the stratospheric aerosol layer state over Tomsk (western Siberia, Russia). *Atmos. Chem. Phys.*, **17**, 3067–3081, https://doi.org/10.5194/acp-17-3067-2017.

Brought to you by NOAA Central Library | Unauthenticated | Downloaded 07/19/23 04:33 PM UTC